IOP Publishing Nanotechnology
Nanotechnology 27 (2016) 154001 (8pp) doi:10.1088/0957-4484/27/15/154001

Plasmon assisted 3D microstructuring of gold nanoparticle-doped polymers

Linas Jonušauskas[1], Marcus Lau[2], Peter Gruber[3], Bilal Gökce[2], Stephan Barcikowski[2], Mangirdas Malinauskas[1] and Aleksandr Ovsianikov[3]

[1] Department of Quantum Electronics, Vilnius University, Saulėtekio Ave. 9, Vilnius LT-10222, Lithuania
[2] University of Duisburg-Essen and Center for Nanointegration Duisburg-Essen (CENIDE), Technical Chemistry I, Universitaetsstr. 7, 45141 Essen, Germany
[3] Institute of Materials Science and Technology (E308), TU-WIEN (Technische Universität Wien), Getreidemarkt 9, 1060 Wien, Austria

E-mail: bilal.goekce@uni-due.de, mangirdas.malinauskas@ff.vu.lt and aleksandr.ovsianikov@tuwien.ac.at

Received 13 November 2015, revised 1 February 2016
Accepted for publication 5 February 2016
Published 29 February 2016

Abstract

3D laser lithography of a negative photopolymer (zirconium/silicon hybrid solgel SZ2080) doped with gold nanoparticles (Au NPs) is performed with a 515 nm and 300 fs laser system and the effect of doping is explored. By varying the laser-generated Au NP doping concentration from $4.8 \cdot 10^{-6}$ wt% to $9.8 \cdot 10^{-3}$ wt% we find that the fabricated line widths are enlarged by up to 14.8% compared to structures achieved in pure SZ2080. While implicating a positive effect on the photosensitivity, the doping has no adverse impact on the mechanical quality of intricate 3D microstructures produced from the doped nanocompound. Additionally, we found that SZ2080 increases the long term (~months) colloidal stability of Au NPs in isopropanol. By discussing the nanoparticle–light interaction in the 3D polymer structures we provide implications that our findings might have on other fields, such as biomedicine and photonics.

Keywords: nanoparticles, laser lithography, plasmons, 3D microstructures, photonics, multi-photon processing, biomedicine

(Some figures may appear in colour only in the online journal)

1. Introduction

The optical properties of gold nanoparticles, namely the surface plasmon resonance, are correlated to size, shape and the surrounding medium [1–3]. The first reports of these optical properties go back to Faraday in 1857 [4]. Until now several potential applications of these particles, e.g. catalysis and biology, have been explored [5]. One way to generate ligand-free gold nanoparticles (Au NPs), besides other well-established synthesis methods such as applying two-phase liquid systems [6], polymer agents [7] and nanosphere lithography [2], is pulsed laser ablation in liquids (PLAL). First reported by Fojtik and Henglein [8], this method is gaining more and more attention. PLAL gives access to a wide range of particle sizes [9] with relevance to e.g. catalysis applications [10]. Due to the possibility of generating the particles in different solvents, they can be transferred easily into polymers if synthesised in a solvent compatible with the target polymer [11–13, 31]. Also, Au NPs fabricated by PLAL show a high colloidal stability due to their surface charge [14, 33]. In this work we modify the optical response of a photopolymer used in 3D laser lithography (3DLL) by integrating plasmonic gold nanoparticles into the polymer.

3DLL is an emerging approach for producing complex 3D micro- and nanostructures from many different materials [15–17]. To date, it is applied to manufacturing structures for many applications, including photonics [18], microoptics [19], micromechanics [20] and biomedicine [21]. Currently, a lot of work is dedicated to improving this technology in order to enhance its flexibility and efficiency [22–24]. One way to achieve this is to improve or adapt the materials used in this technology. In the case of polymers processed using 3DLL, several different options are viable. Additional components can be added to the polymer thus generating modified or new

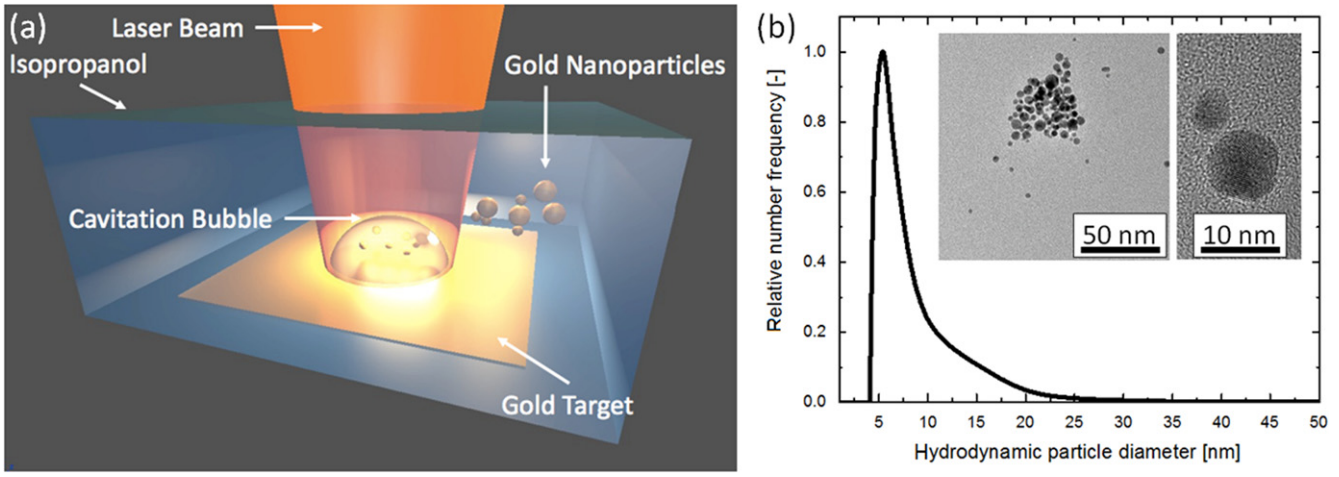

Figure 1. (a) An image depicting relevant entities occurring during pulsed laser ablation in liquids; (b) size distribution of Au NPs generated by laser ablation in isopropanol measured in an analytical disc centrifuge. Insets show HR-TEM images of representative particles.

optical properties of the material [25–27]. Such modifications improve the flexibility of 3DLL, allowing the production of structures from materials that have additional active properties beneficial to the fabricated structure.

The goal of this work was to produce Au NP-doped materials and process them by 3DLL. For this purpose we doped a hybrid organic–inorganic pre-polymer (SZ2080), which is widely used in 3DLL [16, 28], with Au NPs and created various structures from this nanocomposite. Within this experimental study the effect of Au NPs on the materials' photosensitivity was investigated. The influence of Au NPs' presence on the structural quality of complex 3D structures generated by 3DLL was also assessed. Laser structuring of such a nanocomposite could lead to the creation of a unique material with active laser wavelength dependent photonic properties for applications in metamaterials or a material with good laser structuring capabilities and desired active properties for biomedicine.

2. Materials and methods

Au NPs were produced by PLAL [29] (schematically illustrated in figure 1(a)). Such nanoparticles are known to have an improved nanoparticle–polymer coupling due to the ligand-free nanoparticle surface generated during laser ablation [30, 31]. An Nd:YAG laser (Ekspla, Atlantic) with 10 ps pulse duration, 100 kHz repetition rate, 150 μJ pulse energy and 1064 nm laser wavelength was used for fabrication of the Au NPs. The laser beam was directed into a laser scanner and focused with an f-theta lens (focal length of 100.1 mm) on a gold target (99.9%), which was placed in isopropanol in a self-constructed stirred batch chamber. The liquid layer over the target measured 6 mm. The nanoparticles generated by PLAL in isopropanol had a surface charge of ~ -32 mV (measured with a Nicomp 380 ZLS). When the colloid was mixed with the pre-polymer, steric stabilisation took place [32]. This screened the zeta potential value to almost zero charge (~ -1.5 mV). The particle size distribution was measured in an analytical disc centrifuge (CPS instruments) and TEM images (taken with a JEOL JEM-2200FS TEM) of the AU NP are shown in figure 1(b).

PLAL results in charged nanoparticles [33], independent of the pulse duration in the ns, ps or fs regimes. By comparing pulse duration effects it has been shown that while the ns regime is most productive, it may cause thermal decomposition of the solvent [34]. In comparison Zand *et al* have shown that ps lasers are the most efficient for PLAL [34]. Additionally, high repetition rate ps PLAL may lead to post irradiation in batch chambers, causing fragmentation and size reduction [35, 36]. On the other hand it is well established that a white light continuum generated via fs pulses contributes to homogenisation of different sizes of ablated Au NPs [37]. However, ultrashort pulses also lead to degradation of the liquid in nanoparticle colloid synthesis [38] and is neither the most efficient nor productive [34]. The laser parameters affecting nanoparticle size control, stability of laser ablation synthesis and laser fragmentation of gold have recently been reviewed by Rehbock *et al* [9]. The organic solvent isopropanol provides nanoparticle surface adsorbates, resulting in *in situ* size quenching and surface charge delivery via the alcoholate form of the solvent molecule [39].

The Au NPs in isopropanol were mixed with the hybrid organic–inorganic pre-polymer SZ2080 [28] figure 3(a). Mixing of two materials by using a magnetic stirrer is a far simpler approach compared to other attempts to integrate nanoparticles into the pre-polymer for 3D laser fabrication [40]. Concentrations are given as Au NP mass to the mass of pure SZ2080 ($m_{\mathrm{AuNP}}/m_{\mathrm{SZ2080}}$), i.e. when solvent (isopropanol) is removed and ranged from $4.8 \cdot 10^{-6}$ wt% to $9.8 \cdot 10^{-3}$ wt%. Such concentrators were chosen because of relatively easy mixing process with pre-polymer and were sufficient to change the optical properties of the resist by AuNP significantly. Au NPs in isopropanol and Au NPs in SZ2080 extinction spectra (in normalised form) are given in figure 2. SZ2080 as a material was chosen because of the ability to structure it by femtosecond laser pulses in both forms, that is when photosensitised by a photoinitiator (PI) (in

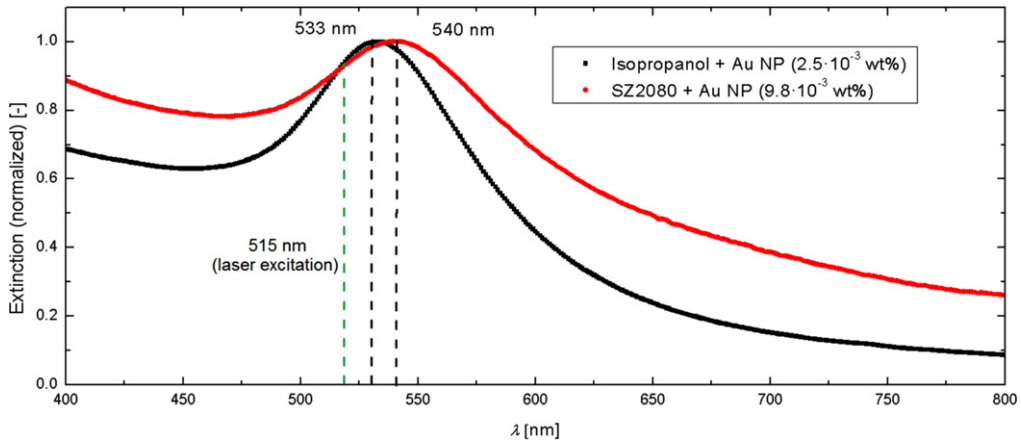

Figure 2. Normalised extinction spectra of Au NPs in isopropanol (peak centred around 533 nm) and SZ2080 doped with Au NPs (peak around 540 nm). Concentrations are $2.5 \cdot 10^{-3}$ wt% and $9.8 \cdot 10^{-3}$ wt%, respectively. Green dashed line—laser wavelength used in this work for excitation (515 nm).

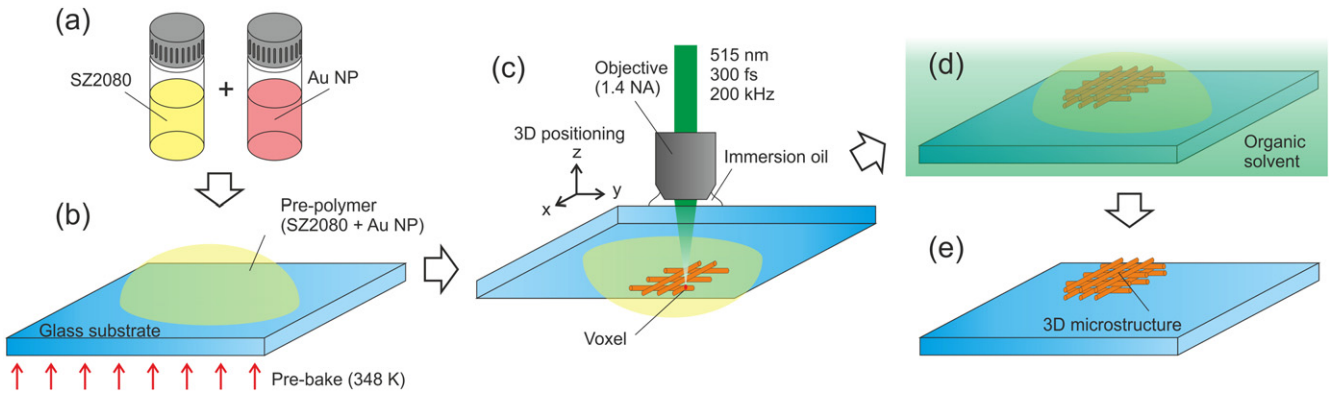

Figure 3. Fabrication steps taken during creation of laser-produced 3D structures: (a) mixing of SZ2080 with Au NPs; (b) pre-bake of the pre-polymer on a glass substrate at 348 K; (c) point-by-point laser manufacturing; (d) development in the organic solvent; (e) finished free-standing 3D structure ready for characterisation/application.

this work Irgacure 369 (IRG)) and when non-photosensitised i.e. in pure resist form [41]. Also, structures produced from this pre-polymer show very low shrinkage, optical transparency in all visible spectra [28] and biocompatibility [42]. Isopropanol in liquid phase was chosen because it shows good colloidal stability for Au NPs and the SZ2080 is soluble in isopropanol. Therefore, the Au NPs previously generated by PLAL can be transferred easily into the pre-polymer by dissolving a defined amount of the material in the gold/isopropanol colloid and by subsequently vaporising the isopropanol. This transfer enables the controlled transition of the Au NPs into the SZ2080 with defined concentrations, which is of particular interest for this study.

SZ2080 samples (doped with varying quantities of Au NPs, PI and in pure form) were prepared by drop-casting the pre-polymer on glass substrates. All samples were pre-baked at 348 K for 45 minutes, thus removing the isopropanol and leaving the Au NP-doped pre-polymer in solid gel form (figure 3(b)). After pre-baking, samples were processed using a femtosecond laser. Samples were attached to positioning system pre-polymer drop facing down thus ensuring a good spread of immersion oil. 3D microstructures were achieved by tightly focusing the femtosecond laser beam into the pre-polymer (figure 3(c)). This led to a high intensity in the focal point which initiated photochemical reactions in the pre-polymer and created a volume pixel (voxel). Material outside the focal point was not affected. Such an approach allows point-by-point free-form true 3D fabrication. A detailed description of the setup used can be found elsewhere [43]. After laser microfabrication the samples were developed in 4-methyl-2-pentanone for 45 minutes (figure 3(d)), thus revealing a produced 3D structure that could be examined or used later (figure 3(e)).

In this work we used a 63× objective with numerical aperture (NA) of 1.4. In all the experiments sample translation velocity was kept at 100 μm s^{-1}. Average laser power (P) was measured as a main laser radiation parameter. P was recalculated into the laser peak intensity I during the pulse at the centre of the focus using the following equation:

$$I = \frac{2PT}{fw^2\pi\tau}, \tag{1}$$

where f is pulse repetition rate, τ is pulse duration and $\omega = 0.61\lambda/\mathrm{NA}$ is the waist (radius) of the beam [22]. T is system transparency (without glass substrate and pre-polymer) which was 0.41 for a 63 × 1.4 NA objective.

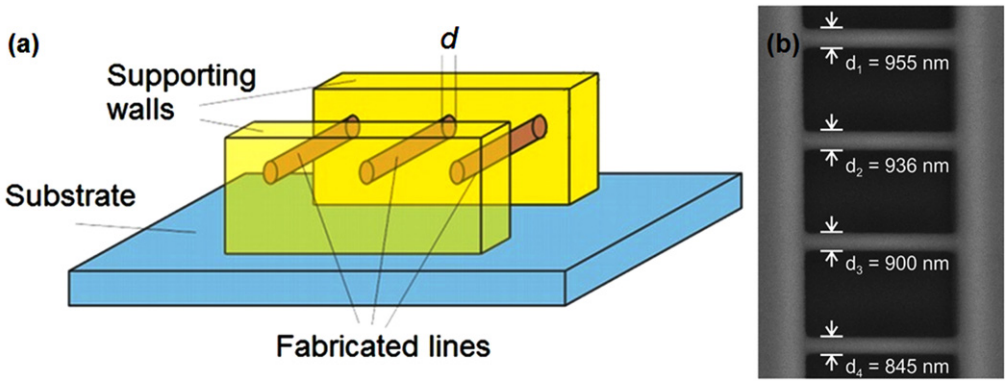

Figure 4. (a) Principle of the spatial resolution measurement using the RB method; (b) SEM micrograph of lines fabricated between supporting walls using varying *I*.

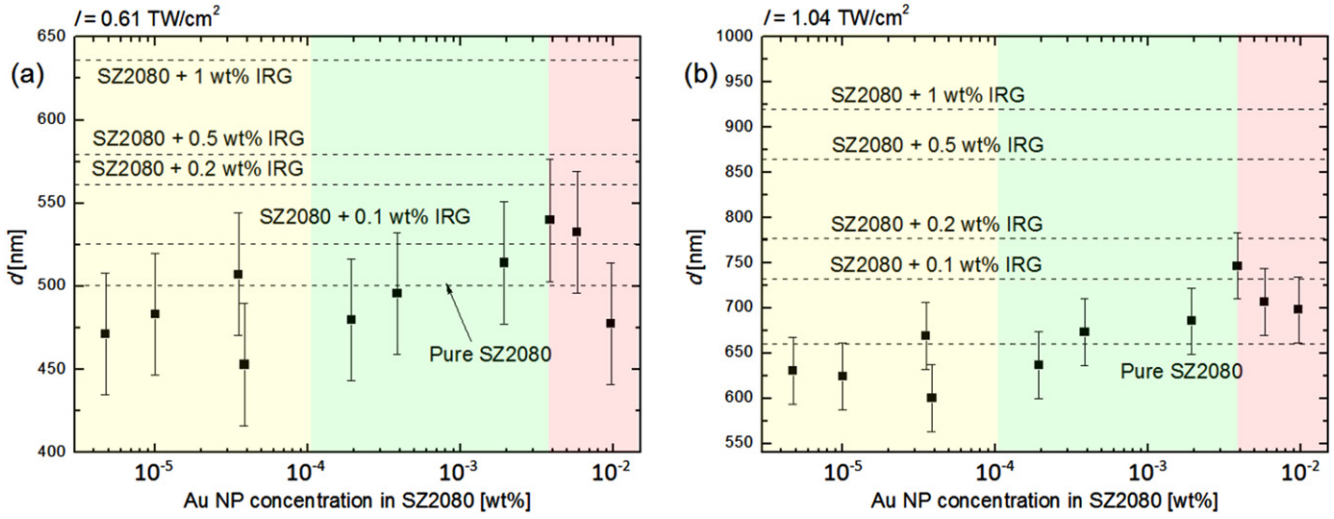

Figure 5. Line widths achieved with different Au NP concentrations when radiation intensity $I = 0.61$ TW cm^{-2} a and $I = 1.04$ TW cm^{-2} (b). These intensities were chosen as the ones that represent the middle (a) and the upper limit of the fabrication window (b). Dashed lines show feature sizes achieved with SZ2080 photosensitised with varying PI amounts and in pure form. The yellow zone represents concentrations in which achieved feature sizes are close to or below that of pure SZ2080. The green zone shows increase in line widths as Au NP concentration rises and the red zone shows saturation of this effect.

After laser structuring, the samples were characterized by scanning electron microscopy (SEM) (Hitachi TM-1000). The spatial resolution of the fabricated features was measured using a resolution bridge (RB) method shown in figure 4(a) [44]. This method is realised as follows: strong supporting walls are fabricated first. Then, individual lines are fabricated perpendicular to supporting walls. Every line is produced with varying *I*. Development reveals lines suspended above the substrate (in our case lines were 7μm above the glass substrate). This way their width *d* can be measured using SEM (figure 4(b)). In our case we measured only the widths of the lines. SEM used to measure it at maximum magnification (10000×) had a single pixel size of around ~18.5 nm. Combined with a not-perfect contrast between lines and background, an unavoidable deviation between measurement and the real result occurs. We assumed these deviations not to be higher than two pixels in SEM photos and, for this reason, in all resolution measurement graphs we used error bars equal to 37 nm.

3. Results

3.1. Gold nanoparticle impact on the photosensitivity of the nanocompound

To investigate the effect of Au NPs on the photosensitivity of the pre-polymer we compared the resulting feature sizes (line widths) in SZ2080 and Au NP compounds, SZ2080 containing commercial PI IRG and in pure SZ2080. As shown in figures 5(a) and (b) the concentration of plasmonic Au NPs has a crucial impact on the response of the resin during laser structuring. This shows that with increase of Au NP content in the resin (from $3.9 \cdot 10^{-5}$ to $3.9 \cdot 10^{-3}$) feature size increases and surpasses that of pure SZ2080 (figures 5(a), (b) green zone). When the concentration of Au NPs is $3.9 \cdot 10^{-3}$ wt% lines are on average 14.8% wider than those obtained in pure SZ2080. We consider such an increase in photosensitivity for sufficient Au NP content in the pre-polymer to be the consequence of excitation of Au NP surface plasmons due to the used laser wavelength of 515 nm (figure 2) [45]. This means

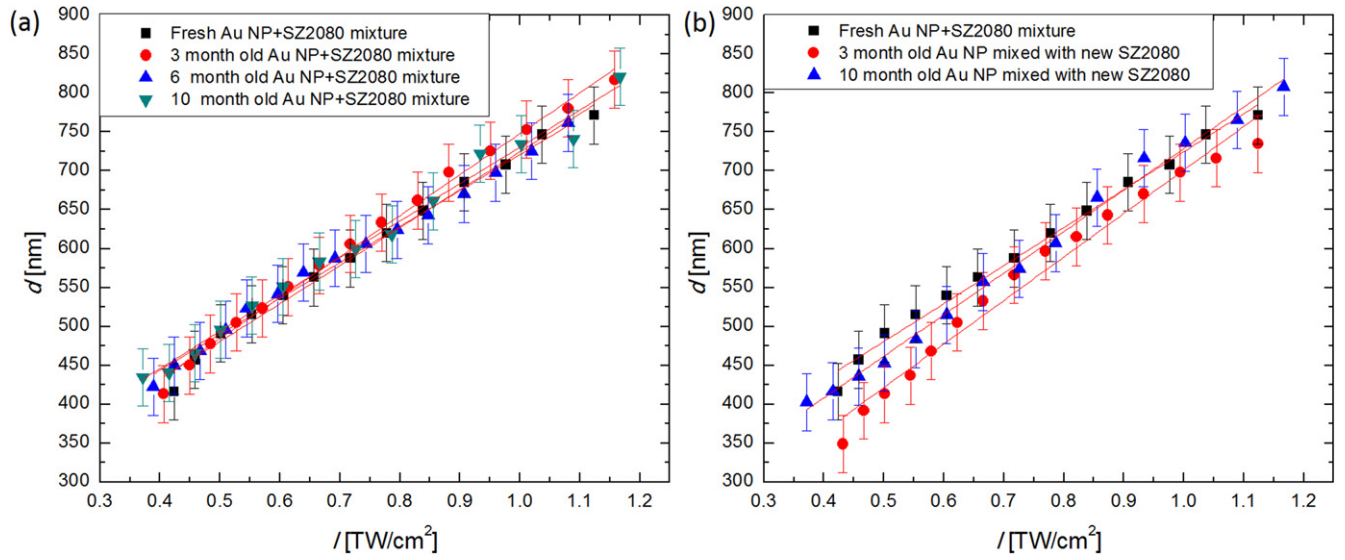

Figure 6. Effect of the Au NP age and stability on the feature size when Au NPs are kept in SZ2080 (a) and separately in standard solvent (b).

that very low concentrations of Au NPs (around 10^{-3} wt%) could act as an agent in the pre-polymer which enhances photosensitivity and increases feature sizes achieved during fabrication, thus allowing us to replace potential toxic PI [46] when its concentration is around or a little above 0.1 wt%.

We would like to point out that line widths achieved with the lower Au NP concentrations show an interesting behaviour in comparison to the pre-polymer with higher Au NP doping. The feature sizes achieved with these nanocompounds are smaller than those of pure SZ2080 (figures 5(a), (b) yellow zone). The lower line width obtained for the lowest Au NP concentrations used here might be explained by plasmonic attenuation of the material. This is in agreement with findings from Lau *et al* [47] during laser structuring. A similar result is obtained when Au NP concentration is above $3.9 \cdot 10^{-3}$ wt% (figures 5(a), (b) red zone). However, this can be attributed to absorption by Au NPs in the path of the laser beam prior to reaching the focal point. In this case, Au NP-enhanced photosensitivity cannot compensate for this absorption. This means that, by varying the Au NP content, the photosensitivity of the material can be both increased and decreased, which would be an interesting topic for further studies in this field.

Further, we studied the detriment of aging of the Au NPs on the photosensitivity. We compared the feature size measurement results of a freshly prepared SZ2080 + Au NP mixture, the same mixture after 3, 6 and 10 months storage time and mixtures that were made from new SZ2080 and 3 month old and 10 month old Au NPs in isopropanol. The results are shown in figures 6(a) and (b). Good colloidal stability of Au NP + SZ2080 mixture after 3, 6 and 10 months is proved by good repeatability of achieved line widths (figure 6(a)). However, if Au NPs are stored in isopropanol without the SZ2080 and materials are prepared after a considerable amount of time (3 or 10 months) the influence on the feature size becomes present (figure 6(b)). Thus, Au NPs and SZ2080 as a mixture have longer-term (up to 10 month) colloidal stability than Au NPs in isopropanol. The improved colloidal stability in the presence of the pre-polymer can be attributed to a stabilizing effect caused by the pre-polymer matrix. Steric stabilisation allows long-term storage and processability, since individual nanoparticles are stabilized by Born repulsion of the macromolecules absorbed on their surface. Hence, ligand-free Au NPs synthesised in isopropanol and their subsequent mixing with a pre-polymer provide a stable educt with dispersed plasmonic nanoparticles, ready for integration into microstructures via 3DLL.

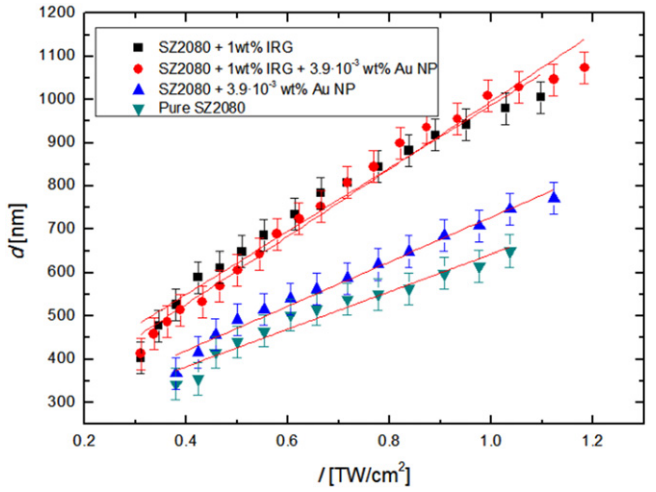

Figure 7. Line widths achieved using SZ2080 containing PI, photosensitised photopolymer doped with Au NPs, pure SZ2080 and SZ2080 doped with Au NPs.

Additionally, the effect of Au NPs on photopolymerisation of resin containing PI was investigated. As shown in figure 7 the presence of Au NPs in photosensitised materials has no observable effect on the photosensitivity. This might be explained by the improved sensitivity caused by the PI that has stronger impact than the plasmonic effect of the Au NPs.

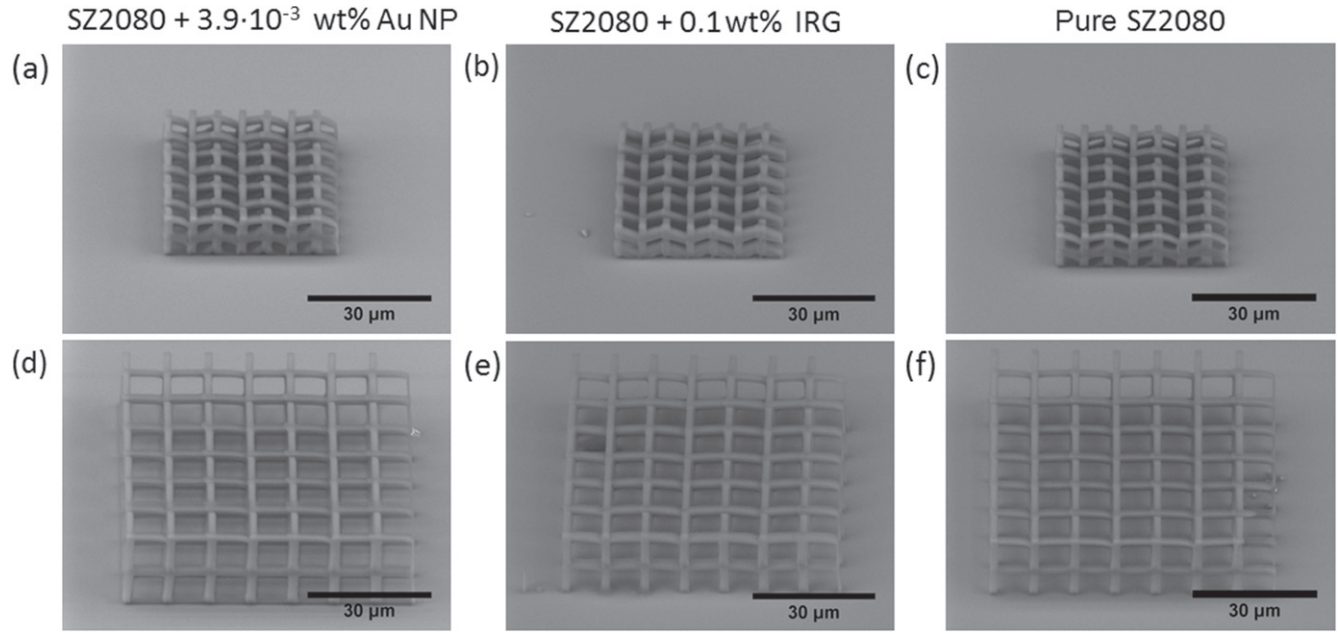

Figure 8. Comparison of structures produced from SZ2080 doped with $3.9 \cdot 10^{-3}$ wt% Au NPs ((a) and (d)), SZ2080 with 0.1 wt% IRG ((b), ((e)) and pure SZ2080 ((c), (f)). Structures produced from the material combining polymer and Au NPs show no defects. $I = 0.61$ TW cm^{-2}.

3.2. 3D structures produced from a polymer doped with gold nanoparticles

In further experiments we produced free-form 3D structures from the nanocompound. We modelled two different 3D structures which differed both in size and internal geometry. For comprehensive comparison the same structures were fabricated from SZ2080 with and without PI. The chosen PI concentration was 0.1 wt% as it represents the concentration of PI that Au NPs can replace. Figure 8 shows SEM images of these structures.

Any imperfection in the structure, such as crack or deformation can be considered as a defect. If such defects were present in the final structure, this would indicate deficiency in the material or an improperly executed fabrication development procedure [48]. It is clear that there are no defects in the structures produced from SZ2080 doped with Au NPs, as seen in figure 8. This means that doping of the resin with Au NPs (at least with concentrations up to $3.9 \cdot 10^{-3}$ wt%) has no negative impact on the quality of fabricated 3D structures with intricate internal geometry.

4. Discussion

The effect demonstrated in this work, i.e. increase in photosensitivity of Au NP-doped pre-polymers can be explained by a plasmonic effect caused by the Au NPs [1, 49–51]. In this study we used a 515 nm laser wavelength, which is close to the surface plasmon resonance wavelength of the Au NPs shown in figure 2, thus they can be sufficiently excited. As shown in figure 5, smaller quantities of Au NPs result in a lower feature diameter, while for higher Au NP concentrations an enhanced photosensitivity can be observed. This is similar to experimental findings from Lau *et al* where the impact of gold nanoparticle concentration on laser sintering was investigated [47]. Also, such nanocomposites can be produced by just simply mixing two substances (Au NPs and a pre-polymer) which is a much simpler approach in comparison to other methods, such as ion implantation [40], used to integrate nanoparticles into a pre-polymer for 3D laser processing.

There may be two research fields that could greatly benefit from findings presented in this work, namely biomedicine [52] and photonics [53]. Research aiming to combine 3DLL and biomedicine is currently gathering a great deal of interest and shows promising results in creating 3D scaffolds for stem cell growth [21, 42]. It was shown that nanoparticles in general can perform many different roles in medicine, such as antibacterial agents [54], helping with magnetic fluid hyperthermia [55] or use for advanced drug or even gene delivery [56]. The inclusion of nanoparticles in polymer structures can lead to active medical implants that have desired properties and biofunctionalisation given by the nanoparticles or even act as a nanoparticle delivery system if the polymer is biodegradable [57]. In addition, photonics could benefit from Au NPs in polymers as well. Currently 3DLL-produced photonic crystals allow controlling light due to the shape and internal structure of such photonic device [58]. We suggest that by adding Au NPs an to already intricate 3D structure we could unlock an entirely new level of photonic tunability and pave the way to the creation of an entirely new generation of 3D-nanodoped photonic devices in which desired properties are achieved through the combination of both internal 3D structure and smart placement of Au NPs inside such a structure [26].

However, at this point there are still further questions concerning Au NPs and femtosecond laser light interaction in pre-polymers that should be answered. We attributed the

increase in photosensitivity to amplified plasmonic effects caused by Au NPs in the focal point, but at this point we are not sure if this is a complimentary effect that only supports photochemical reaction that has already been started by other effects (for example multiphoton absorption or avalanche ionisation [41, 45]) or it actually initiates photochemical reactions. Finally, other nanocompounds containing other polymers commonly used in 3DLL should be tested. These studies will be performed in the near future.

5. Conclusions

The presented results show that mixing the hybrid organic–inorganic polymer SZ2080 with 7 nm Au NPs increases long-term (up to 10 months) colloidal stability of the nanoparticles with respect to their aging in isopropanol as produced by PLAL. Doping up to a concentration of $3.9 \cdot 10^{-3}$ wt% enlarges 3DLL fabricated line widths by up to 14.8% compared to pure material. This suggests that it can replace up to 0.1 wt% of commercial photoinitiator Irgacure 369 in SZ2080 in terms of photosensitivity. Finally, the manufactured 3D microstructures of such a nanocompound showed no detectable deviations of geometrical integrity. This knowledge can be used as a base for future work aimed at further examining mechanisms in pulsed laser processing of NP-doped polymers. Furthermore, functional devices with exotic properties granted by a combination of 3D micro-architecture and Au NPs can be realized by 3DLL and potentially applied in novel photonic devices and biomedical scaffolds, to mention a few potential applications.

Acknowledgments

We acknowledge ECs Seventh Framework Programme Laserlab-Europe IV JRA support BIOAPP (EC-GA 654148). We also thank Friedrich Waag (University of Duisburg-Essen) for the TEM-measurements.

References

[1] Jain P K, Huang X, El-Sayed I H and El-Sayed M A 2007 Review of some interesting surface plasmon resonance-enhanced properties of noble metal nanoparticles and their applications to biosystems *Plasmonics* **2** 107–18

[2] Eustis S and El-Sayed M A 2006 Why gold nanoparticles are more precious than pretty gold: Noble metal surface plasmon resonance and its enhancement of the radiative and nonradiative properties of nanocrystals of different shapes *Chem. Soc. Rev.* **35** 209–17

[3] Maier S A and Atwater H A 2005 Plasmonics: Localization and guiding of electromagnetic energy in metal/dielectric structures *J. Appl. Phys.* **98** 011101

[4] Faraday M 1857 The bakerian lecture: experimental relations of gold (and other metals) to light *Phil. Trans. R. Soc. Lond.* **147** 145–81

[5] Daniel M-C and Astruc D 2004 Gold nanoparticles: Assembly, supramolecular chemistry, quantum-size-related properties, and applications toward biology, catalysis, and nanotechnology *Chem. Rev.* **104** 293–346

[6] Brust M, Walker M, Bethell D, Schiffrin D J and Whyman R 1994 Synthesis of thiol-derivatised gold nanoparticles in a two-phase liquid-liquid system *Chem. Commun.* **7** 801–2

[7] Turkevich J, Stevenson P and Hillier J 1951 A study of the nucleation and growth process in the synthesis of colloidal gold *Discuss Faraday Soc.* **11** 55–75

[8] Fojtik A and Henglein A 1993 Laser ablation of films and suspended particles in a solvent: formation of cluster and colloid solutions *Ber. Bunsenges. Phys. Chem.* **97** 252–4

[9] Rehbock C, Jakobi J, Gamrad L, van der Meer S, Tiedemann D, Taylor U, Kues W, Rath D and Barcikowski S 2014 Current state of laser synthesis of metal and alloy nanoparticles as ligand-free reference materials for nano-toxicological assays *Beilstein J. Nanotechnol* **5** 1523–41

[10] Marzun G, Nakamura J, Zhang X, Barcikowski S and Wagener P 2015 Size control and supporting of palladium nanoparticles made by laser ablation in saline solution as a facile route to heterogenous catalysts *Appl. Surf. Sci.* **348** 75–84

[11] Thareja R K and Shukla S 2007 Synthesis and characterization of zinc oxide nanoparticles by laser ablation of zinc in liquid *Appl. Surf. Sci.* **253** 8889–95

[12] Maximova K, Aristov A, Sentis M and Kabashin A V 2015 Size-controllable synthesis of bare gold nanoparticles by femtosecond laser fragmentation in water *Nanotechnology* **26** 065601

[13] Yagyu H and Kikitsu T 2015 Particle size dependence of the laser microfabrication of gold nanoparticles dispersed in polymer resists *J. Micromech. Microeng.* **25** 125018

[14] Sylvestre J-P, Poulin S, Kabashin A, Sacher E, Meunier M and Luong J 2004 Surface chemistry of gold nanoparticles produced by laser ablation in aqueous media *J. Phys. Chem.* B **108** 16864–9

[15] Cheng K and Sugioka Y 2014 Femtosecond laser three-dimensional micro- and nanofabrication *Appl. Phys. Rev.* **1** 041303

[16] Malinauskas M, Žukauskas A, Hasegawa S, Hayasaki Y, Mizeikis V, Buividas R and Juodkazis S 2016 Ultrafast laser processing of materials: from science to industry *Light: Sci. Appl.* in press

[17] Ovsianikov A, Mironov V, Stampfl J and Liska R 2012 Engineering 3D cell-culture matrices: multiphoton processing technologies for biological and tissue engineering applications *Expert Rev. Med. Devices* **9** 613–33

[18] Straub M, Nguyen L H, Fazlic A and Gu M 2004 Complex-shaped three-dimensional microstructures and photonic crystals generated in a polysiloxane polymer by two-photon microstereolithography *Opt. Mater.* **27** 359–64

[19] Malinauskas M *et al* 2012 3D microoptical elements formed in a photostructurable germanium silicate by direct laser writing *Opt. Laser Eng.* **50** 1785–8

[20] Schizas C, Melissinaki V, Gaidukevičiūtė A, Reinhardt C, Ohrt C, Dedoussis V, Chichkov B N, Fotakis C, Farsari M and Karalekas D 2010 On the design and fabrication by two-photon polymerization of a readily assembled micro-valve *Int. J. Adv. Manuf. Technol.* **48** 435–41

[21] Danilevičius P, Rezende P A, Pereira F D A S, Selimis A, Kasyanov V, Noritomi P Y, Silva J V L , Chatzinikolaidou M, Farsari M and Mironov V 2015 Burr-like, laser-made 3D microscaffolds for tissue spheroid encagement *Biointerphases* **10** 021011

[22] Jonušauskas L, Rekštytė S and Malinauskas M 2014 Augmentation of direct laser writing fabrication throughput for three-dimensional structures by varying focusing conditions *Opt. Eng.* **53** 125102

[23] Obata K, Koch J, Hinze U and Chichkov B N 2010 Multi-focus two-photon polymerization technique based on individually controlled phase modulation *Opt. Express* **18** 17193–200

[24] Lim C S, Hong M H, Lin Y, Xie Q and Lukyanchuk B S 2006 Microlens array fabrication by laser interference lithography

for super-resolution surface nanopatterning *Appl. Phys. Lett.* **89** 191125
[25] Žukauskas A, Malinauskas M, Kontenis L, Purlys V, Paipulas D, Vengris M and Gadonas R 2010 Organic dye doped microstructures for optically active functional devices fabricated via two-photon polymerization technique *Lith. J. Phys.* **50** 55–61
[26] Li J, Jia B, Zhou G and Gu M 2006 Fabrication of three-dimensional woodpile photonic crystals in a Pbse quantum dot composite material *Opt. Express* **14** 10740
[27] Ushiba S, Shoji S, Masui K, Kono J and Kawata S 2014 Direct laser writing of 3D architectures of aligned carbon nanotubes *Adv. Mater.* **26** 5653–7
[28] Ovsianikov A *et al* 2008 Ultra-low shrinkage hybrid photosensitive material for two-photon polymerization microfabrication *ACS Nano* **2** 2257–62
[29] Lau M, Ziefuss A, Komossa T and Barcikowski S 2015 Inclusion of supported gold nanoparticles into their semiconductor support *Phys. Chem. Chem. Phys.* **17** 29311–8
[30] Barcikowski S, Baranowski T, Durmus Y, Wiedwald U and Gökce B 2015 Solid solution magnetic FeNi nanostrand-polymer composites by connecting-coarsening assembly *J. Mater. Chem.* C **3** 10699–704
[31] Zhang D and Barcikowski S 2015 Rapid nanoparticle-polymer composite prototyping by laser ablation in liquids *Encyclopedia of Polymeric Nanomaterials* ed S Kobayashi and S Müllen 2131–2141 (Berlin: Springer) pp 2131–41
[32] Streich C, Koenen S, Lelle M, Peneva K and Barcikowski S 2015 Influence of ligands in metal nanoparticle electrophoresis for the fabrication of biofunctional coatings *Appl. Surf. Sci.* **348** 92–9
[33] Merk V, Rehbock C, Becker F, Hagemann U, Nienhaus H and Barcikowski S 2014 In situ non-DLVO stabilization of surfactant-free, plasmonic gold nanoparticles: Effect of hofmeister's anions *Langmuir* **30** 4213–22
[34] Zand D D, Nachev P, Rosenfeld R, Wagener P, Pich A, Klee D and Barcikowski S 2012 Nanocomposite fibre fabrication via *in situ* monomer grafting and bonding on laser-generated nanoparticles *J. Laser Micro. Nanoeng.* **7** 21–7
[35] Schwenke A, Wagener P, Nolte S and Barcikowski S 2011 Influence of processing time on nanoparticle generation during picosecond-pulsed fundamental and second harmonic laser ablation of metals in tetrahydrofuran *Appl. Phys.* A **104** 77–82
[36] Lau M, Haxhiaj I, Wagener P, Intartaglia R, Brandi F, Nakamura J and Barcikowski S 2014 Ligand-free gold atom clusters adsorbed on graphene nano sheets generated by oxidative laser fragmentation in water *Chem. Phys. Lett.* **610-611** 256–60
[37] Kubiliūtė R *et al* 2013 Ultra-pure, water-dispersed Au nanoparticles produced by femtosecond laser ablation and fragmentation *Int. J. Nanomedicine* **8** 2601–11
[38] Besner S, Kabashin A V, Winnik F M and Meunier M 2009 Synthesis of size-tunable polymer-protected gold nanoparticles by femtosecond laser-based ablation and seed growth *J. Phys. Chem.* C **113** 9526–31
[39] Cristoforetti G, Pitzalis E, Spiniello R, Ishak R, Giammanco F, Muniz-Miranda M and Caporali S 2012 Physico-chemical properties of Pd nanoparticles produced by pulsed laser ablation in different organic solvents *Appl. Surf. Sci.* **258** 3289–97
[40] Stepanov A L, Kiyan R, Ovsianikov A, Nuzhdin V I, Valeev V F, Osin Y N and Chichkov B N 2012 Synthesis and optical properties of silver nanoparticles in ORMOCER *Appl. Phys.* A **108** 375–8
[41] Malinauskas M, Žukauskas A, Bičkauskaitė G, Gadonas R and Juodkazis S 2010 Mechanisms of three-dimensional structuring of photo-polymers by tightly focussed femtosecond laser pulses *Opt. Express* **18** 10209
[42] Malinauskas M *et al* 2012 In vitro and *in vivo* biocompatibility study on laser 3D microstructurable polymers *Appl. Phys.* A **108** 751–9
[43] Malinauskas M, Kiršanskė G, Rekštytė S, Jonavičius T, Kaziulionytė E, Jonušauskas L and Žukauskas A 2012 Nanophotonics lithography: a versatile tool for manufacturing functional three-dimensional micro-/nano-objects *Lith. J. Phys.* **52** 312–26
[44] Malinauskas M, Danilevičius P and Juodkazis S 2011 Three-dimensional micro-/nanostructuring via direct write polymerization with picosecond laser pulses *Opt. Express* **19** 5602–10
[45] Smirnov A, Pikulin A, Sapogova N and Bityurin N 2014 Femtosecond laser irradiation of plasmonic nanoparticles in polymer matrix: Implications for photothermal and photochemical material Alteration *Micromachines* **5** 1202–18
[46] Benedikt S, Wang J, Markovic M, Moszner N, Dietliker K, Ovsianikov A, Grotzmacher H and Liska R 2016 Highly efficient water-soluble visible light photoinitiators *J. Polym. Sci.* **54** 473–9
[47] Lau M, Niemann R G, Bartsch M, O'Neill W and Barcikowski S 2014 Near-field-enhanced, off-resonant laser sintering of semiconductor particles for additive manufacturing of dispersed Au-ZnO-micro/nano hybrid structures *Appl. Phys.* A **114** 1023–30
[48] Cicha K, Stadlmann K, Li Z, Ovsianikov A, Markut-Kohl R, Liska R and Stampfl J 2011 Evaluation of 3D structures fabricated with two-photon-photopolymerization by using FTIR spectroscopy *J. Appl. Phys.* **110** 064911
[49] Ueno K, Juodkazis S, Shibuya T, Yokota Y, Mizeikis V, Sasaki K and Misawa H 2008 Nanoparticle plasmon-assisted two-photon polymerization induced by incoherent excitation source *J. Am. Chem. Soc.* **130** 6928–9
[50] Ueno K, Juodkazis S, Shibuya T, Mizeikis V, Yokota Y and Misawa H 2009 Nanoparticle-enhanced photopolymerization *J. Phys. Chem.* C **113** 11720–4
[51] Murazawa N, Ueno K, Mizeikis V, Juodkazis S and Misawa H 2009 Spatially selective nonlinear photopolymerization induced by the near-field of surface plasmons localized on rectangular gold nanorods *J. Phys. Chem.* C **113** 1147–9
[52] Giljohann D A, Seferos D S, Daniel W L, Massich M D, Patel P C and Mirkin C A 2010 Gold nanoparticles for biology and medicine *Angew. Chem. Int. Ed. Engl.* **49** 3280–94
[53] Zhang X, Sun B, Friend R H, Guo H, Nau D and Giessen H 2006 Metallic photonic crystals based on solution-processible gold nanoparticles *Nano Lett.* **6** 651–5
[54] Thirumalairaj V K, Vijayan M P, Durairaj G, Shanmugaasokan L, Yesudas R and Gunasekaran S 2014 Potential antibacterial activity of crude extracts and silver nanoparticles synthesized from Sargassum wightii *Int. Curr. Pharm. J.* **3** 322–5
[55] Latorre M and Carlos R 2009 Applications of magnetic nanoparticles in medicine: magnetic fluid hyperthermia *Proc. R. Health Sci. J.* **28** 227–38
[56] Mamaeva V, Sahlgren C and Linden M 2013 Mesoporous silica nanoparticles in medicine-Recent advances *Adv. Drug Deliv. Rev.* **65** 689–702
[57] Ulbricht J, Jordan R and Luxenhofer R 2014 On the biodegradability of polyethylene glycol, polypeptoids and poly(2-oxazoline)s *Biomaterials* **35** 4848–61
[58] Maigytė L and Staliūnas K 2015 Spatial filtering with photonic crystals *Appl. Phys. Rev.* **2** 011102